magnetochemistry

MDPI

Article

PAN—Composite Electrospun-Fibers Decorated with Magnetite Nanoparticles

Zulkhair Mansurov [1,2], Gaukhar Smagulova [1,2], Bayan Kaidar [1,2], Aigerim Imash [1,2,*] and Aidos Lesbayev [1,3]

[1] Institute of Combustion Problems, Almaty 050012, Kazakhstan
[2] The Faculty of Chemistry and Chemical Technology, Al-Farabi Kazakh National University, Almaty 050040, Kazakhstan
[3] Department of "General Physics", Satbayev University, Almaty 050000, Kazakhstan
* Correspondence: iimash.aigerim@gmail.com; Tel.: +7-708-904-1229

Abstract: The results of the synthesis of PAN(polyacrylonitrile)-magnetite composite fibers using the electrospinning method are presented. The electrospinning installation included a rotating drum collector for collecting fibers. Magnetite nanoparticles were synthesized using chemical condensation from an iron chloride solution. It was shown that homogeneous Fe_3O_4 magnetite nanoparticles with particle sizes of 6–16 nm could be synthesized using this method. Magnetite nanoparticles were investigated using X-ray diffraction analyses and transmission electron microscopy. Based on magnetite nanoparticles, composite PAN/magnetite fibers were obtained through electrospinning. The obtained composite fibers were investigated using scanning electron microscopy, X-ray diffraction analyses, and elemental analyses. It was shown that the magnetite nanoparticles were uniformly distributed on the surface of the fibers. A comparison of PAN fibers without any added magnetite to PAN/magnetite fibers showed that the addition of magnetite led to a decrease in the value of the fiber diameter at the same polymer concentration and under the same electrospinning process conditions.

Keywords: magnetite; electrospinning; polyacrylonitrile; composite fibers

Citation: Mansurov, Z.; Smagulova, G.; Kaidar, B.; Imash, A.; Lesbayev, A. PAN—Composite Electrospun-Fibers Decorated with Magnetite Nanoparticles. *Magnetochemistry* **2022**, *8*, 160. https://doi.org/10.3390/magnetochemistry8110160

Academic Editor: Xiaojun Zeng

Received: 23 October 2022
Accepted: 15 November 2022
Published: 21 November 2022

1. Introduction

The magnetic properties of materials are used in science and technology, including acoustic systems, proximity sensors [1], electric machines [2], magnetic separators [3], cell phones, cameras, etc [4–7]. Magnetic nanomaterials play an important role in nanomedicine and have led to the development of new methods of magnetic diagnostics, such as magneto resistive and microhall (μHall) biosensors, magnetic particle spectroscopy, etc. Magnetic nanoparticles are also used as contrast agents in magnetic resonance tomography and as indicator materials in magnetic particle imaging [8].

Transitioning to the nanoscale has led to the formation of a new direction in the science of magnetic materials: magnetic nanomaterials. The composition, structure, and properties of magnetic nanomaterials vary widely and depend on the starting materials, synthesis methods, and practical tasks they are aimed at solving. Most commonly, magnetic nanomaterials are synthesized from Ni, Co, and Fe. Among magnetic nanomaterials, Fe-based compounds occupy a leading position, especially Fe_3O_4 magnetite.

According to the classification of nanomaterials based on their geometrical and structural characteristics, magnetic nanomaterials can have a 0D (zero-dimensional) structure, such as magnetic nanoparticles and nanopowders. The review [9] represents the methods used in the synthesis of magnetic nanoparticles, 90% of which are chemical methods. The issues related to nanoparticle modification by organic and inorganic compounds, polymers, and bioactive molecules are discussed. Further, methods of protein immobilization using magnetic nanoparticles, mainly based on Fe_3O_4, are discussed. There are methods of achieving the simultaneous synthesis of Fe_3O_4 and Co_3O_4 oxides mixtures within the flame [10]. Further, based on magnetite nanoparticles, the "core-shell" type structures

are created. In paper [11], the synthesis of the Fe_3O_4/SiO_2 and $CoFe_2O_4/SiO_2$ structures through co-precipitation or the hydrothermal synthesis of Fe_3O_4 was shown. The obtained Fe_3O_4 was a coated surface with a layer of silicon dioxide, and functionalization was carried out with 3-aminopropyl-triethoxysilane. The reduction in the saturation magnetization of the magnetic cores was achieved through coating formation and functionalization [12]. Various magnetite-based core-shell structures are also presented in the review [13]. One of the most intensively developing areas is the production of magnetic fluids, and recently, magnetic nanofluids, including those based on magnetite nanoparticles [14].

One-dimensional (1D) structures include magnetic nanofibers, nanorods, nanotubes, and other one-dimensional configurations. In paper [15], a method of obtaining oriented porous fibers from magnetite (>96% yield) using hydrothermal methods in an aqueous solution of citric acid with a protein addition was proposed. The obtained magnetite fibers have a cylindrical shape with a diameter of 120 nm and are characterized by their porous structure, with a pore size of <5 nm and a high specific surface area (123 m^2/g). The influence of synthesis conditions on the structure of the obtained fibers was studied. The possibility of the application of magnetic fibers as an effective adsorbent for the removal of some toxic chemical substances on the example of Cr(VI) (anions), Hg(II) (cations), and polychlorinated biphenyl (non-polar molecules) was shown.

In addition to obtaining fibers from pure magnetite, many studies have been devoted to obtaining magnetite-based nanofibers [16,17]. In paper [18], the results of the synthesis of PAN/Fe_3O_4 magnetic nanofibers using the electrospinning method are presented. The authors synthesized Fe_3O_4 nanoparticles with an average diameter of about 8 nm. Three concentrations of polyacrylonitrile (PAN, from 8 to 14 wt. %) were used to study the effect of PAN concentration on the diameter and morphology of PAN/Fe_3O_4 nanofibers. Spherical nanoparticles were formed on the fiber's surface, and the number of spheres gradually decreased with the increasing PAN fraction. When the PAN content exceeded 14 wt. %, no formation of spherical particles was observed in the products. The effect of the addition of LiCl to the PAN solution on the structure of the obtained fibers was also considered.

In [19] the authors synthesized PAN/magnetite fibres by electrospinning method. PAN solution with 14% concentration was prepared in dimethyl sulphoxide at a mass ratio of PAN to magnetite of 1.0:1.8 respectively, and the diameter of magnetite nanoparticles was 50–100 nm in the range. As a result, fibers with an average diameter of 100 ± 45 nm were obtained. Many globular structures were observed within their structure. The authors studied the magnetic properties of PAN/magnetite fibers after electrospinning, stabilization, and carbonization at temperatures of 500 and 800 °C. It was shown that their magnetic properties (hysteresis loop, coercive field) change, which may be explained by a change in the distance between individual particles after stabilization and carbonization and, as consequence, the strengthening of the influence of the particles on one another. Various additives in the composition of the PAN fibers affect the structure at the stage of formation, as well as the processes of further processing. In [20], the effect of 1–10 wt. % of Fe/FeO nanoparticle additives on the structure of PAN fibers after electrospinning and during the stabilization and carbonization processes was investigated. The authors paid much attention to the study of the carbonization process. The influence of the temperature, heating rate, holding time, and cooling rate during carbonization on the structure of the final PAN and Fe/FeO carbon fibers is shown.

An important task is to obtain oriented or ordered magnetic fibers. Thus, in paper [21], the preparation of partially oriented PAN/magnetite magnetic nanofibers on the partially conductive substrates of polypropylene and copper tape is reported. In addition to classical electrospinning, a new direction—bubble electrospinning—is being developed; some features and examples of its implementation are presented in papers [22,23].

Two-dimensional (2D) structures—nanofilms, nanocoatings, nanosheets, etc.—are being actively studied. Hybrid films based on sisal cellulose and magnetite nanoparticles were obtained in [16]. Magnetite nanoparticles of a spherical shape, with an average diam-

eter of 5.1 ± 0.5 nm, were coated with oleic acid and oleylamine to prevent agglomeration. The strength characteristics, elastic modulus, and magnetization of the films were also determined. The influence of magnetite nanoparticles on the formation of polystyrene-block-poly (N-isopropylacrylamide)/magnetite magnetic films was discussed in detail in paper [24]. Films were obtained using the spray coating method. It was shown that, during the initial stage of spray coating, the film containing 2 wt. % of magnetite demonstrated a faster process of complete coating formation compared to the reference. The films exhibit superparamagnetic properties, which make them suitable for magnetic sensors or information storage.

Three-dimensional (3D) structures include a new achievement in the area of aerogels—magnetic oxide-ceramic aerogel [25]. It is characterized by an ultralow density of 55 mg/mL and contains up to 98.7% air. A detailed description of the aerogel formation mechanism is provided, and the superparamagnetic and other properties of the material are considered. Paper [26] details obtaining magenta aerogels based on magnetite nanoparticles through freeze-drying Janus emulsion gels based on olive and silicone oils containing gelatin and sodium carboxymethylcellulose. The obtained aerogels are relevant for smart supercapacitors, biosensors, sorption, and the separation of oil spills. The morphology of the final structure was investigated depending on the initial compositions. In paper [27], the results of Mössbauer's studies of magnetic polymer nanocomposites based on magnetite and polyvinyl alcohol were presented. For this purpose, a polymeric nanocomposite, based on Fe_3O_4 and polyvinyl alcohol (PVA), was synthesized using chemical coprecipitation from $FeCl_3 \cdot 6H_2O$ and $FeCl_2 \cdot 4H_2O$ (2:1). The amount of pure iron in the mixture was varied from 30 to 60 wt. %. It was shown that the nanocomposite based on magnetite and PVA represents separate phases: a magnetic component close to the stoichiometric composition of magnetite, a superparamagnetic nonstoichiometric component, and an intermediate weakly magnetic superposition component.

Magnetite and composites based on it have found their application or are promising for several practical applications. In particular, the shielding properties of concrete with the addition of magnetite nanoparticles were studied in paper [28] and showed better protection against microwave radiation in the frequency range from 0.7 to 13 GHz. The maximum electromagnetic interference suppression efficiency was 19.9 dB at 1.5 GHz, with a thickness of 10 mm and a magnetite content of 0.5 wt. % in the concrete.

The aim of this work was to synthesize composite fibers with magnetic properties. To achieve this, the tasks of synthesizing magnetite nanoparticles and obtaining composite fibers based on PAN with additives of magnetite nanoparticles were set. The novelty and practical significance of the work lie in the development of a method of chemical condensation for the synthesis of nanoparticles with a small dispersion in diameter and obtaining nanofibers from PAN with a uniform distribution of magnetite nanoparticles on the fiber surface through electrospinning.

2. Experimental Part

2.1. Synthesis of Fe_3O_4 Magnetite Nanoparticles

Magnetite Fe_3O_4 nanoparticles were synthesized through chemical condensation according to earlier work [29]. For this purpose, the following were prepared: an aqueous solution of iron (III) chloride hexahydrate ($FeCl_3 \cdot 6H_2O$) at a concentration of 0.32 mol/L and iron sulfate heptahydrate ($FeSO_4 \cdot 7H_2O$) at a concentration of 0.2 mol/L. Aqueous solutions of iron salts, each 325 mL in volume, were poured into a heat-resistant flask, stirred with a heated magnetic stirrer (ISOLAB), and 200 mL of a 25% aqueous ammonia solution ($NH_4OH \cdot H_2O$) were gradually added at a rate of 1 drop/s. The temperature of the aqueous iron salt solution was maintained at 50 °C. The chemical reaction of the formation of magnetite nanoparticles was as follows:

$$FeSO_4 \cdot 7H_2O + 2FeCl_3 \cdot 6H_2O + 8NH_3 \cdot H_2O \rightarrow Fe_3O_4\downarrow + 6NH_4Cl + (NH_4)_2SO_4 + 23H_2O$$

Magnetite nanoparticles were extracted from the solution with a permanent magnet, washed several times with water to neutralize the reaction, and then dried under normal conditions.

2.2. Preparation of PAN/Fe_3O_4 Solution and Obtaining of Composite Fibers

Polyacrylonitrile (with a molecular weight of 150,000 g/mol, DFL Minmet Refractories Corp., Shijiangzhuang City, China) was used as the main fiber-forming polymer. For this purpose, PAN and dimethylformamide (DMF, $(CH_3)_2NC(O)H$, 99.9%, Sigma-Aldrich, Darmstadt, Germany) were mixed at a ratio of 7:93 (wt.) with further homogenization for 2 h on a magnetic stirrer at a stirring speed of 100 rpm and a temperature of 70 °C. After the solution was completely homogenized, the prepared PAN solution was mixed with small portions of magnetite at a ratio of 20:1 (wt.). The suspension was placed in an ultrasonic bath (Grad Technology, Moscow, Russia) for 1 h at 30 °C to achieve uniform distribution of the magnetite nanoparticles in the polymer solution. To obtain composite PAN/Fe_3O_4 fibers, the electrospinning method was used. The schematic diagram of the unit is shown in Figure 1 [30].

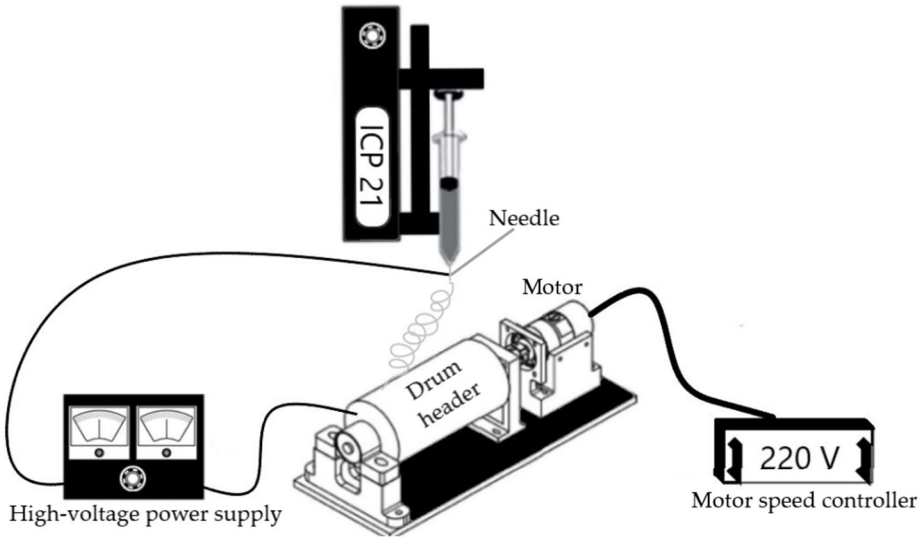

Figure 1. Scheme of the electrospinning system.

The obtained PAN/Fe_3O_4 solution was filled into a 5 mL syringe. The electrospinning process was performed at an ambient temperature of 20–30 °C and a humidity level of 30–50%; the voltage was 12–15 kV, the feed rate was 1.0 mL/h, the feed current was 20 mA, the collector radius was 23 cm, the distance between the needle and collector was 12–15 cm, and the collector surface was covered with aluminum foil for nanofiber deposition (Figure 1).

2.3. Analytical Methods of Investigation for Fe_3O_4 Magnetite Nanoparticles and Composite Fibers

The Fe_3O_4 nanoparticles were examined on the MiniFlex300/600 diffractometer (Rigaku Corp., Tokyo, Japan) and the JEM-1011 transmission electron microscope (TEM) (JEOL, Tokyo, Japan). Scanning electron microscopy (SEM) was completed using the "Quanta 200i 3D" (FEI Company, Peabody, MA, USA) device with a built-in system of energy-dispersive spectroscopy (EDS) and a cryogenic vibrating sample magnetometer. The composite fibers PAN/Fe_3O_4 were investigated through X-ray diffraction analysis (XRD) (using the diffractometer DRON-4M (NPO "Burevestnik", St. Petersburg, Russia) and SEM. For the study of the samples through XRD, the following shooting settings were used: an X-ray tube voltage of 30 kV, tube current of 30 mA, and the step motion of the goniometer at 0.05° 2θ, while measuring the intensity of the point up to 1.0. The rotational speed of the sample in its own plane was 60 rev/min. The processing of radio-

graphs to determine the angular position and intensity of the reflection was carried out using the «Fpeak» program. The phase analysis used the «PCPDFWIN» program from the PDF-2 diffractometric database. The obtained spectra were identified using the JCPDS X-ray database.

3. Results and Discussion

Magnetite nanoparticles were surveyed using XRD, SEM, TEM, and EDS methods and a magnetometer. Figure 2 shows the SEM image, TEM image, and particle size distribution based on the TEM of the magnetite synthesized through chemical deposition. The obtained magnetite nanoparticles were characterized by a small variation in diameter. The predominant fraction of particles had sizes ranging from 6 to 16 nm, with the average size of the particles being 12.22 nm.

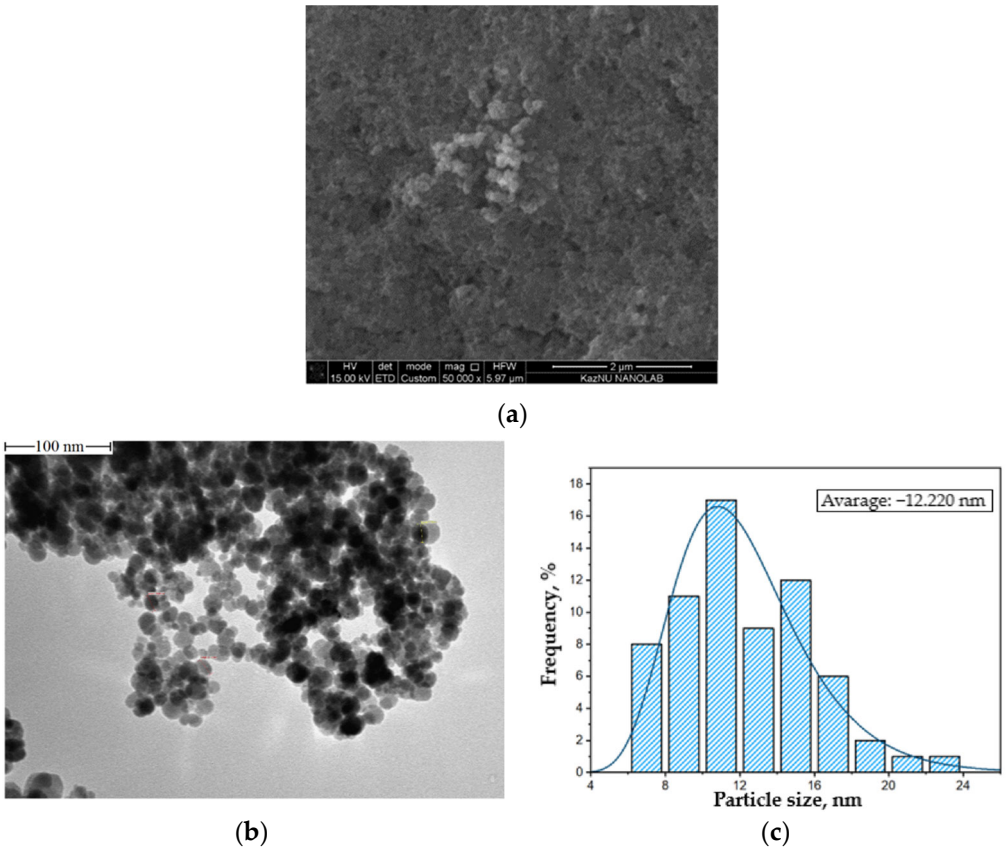

Figure 2. Characterization of magnetite nanoparticles: (**a**) SEM image; (**b**) TEM image; (**c**) particle size distribution based on TEM.

Particles of 50 nm and larger are also provided in the image, but the authors believe that these dimensions are due to the overlapping of the particles. The agglomeration of magnetic particles is due to the presence of high surface energy between the prepared magnetic nanoparticles and the presence of magnetic dipole–dipole interactions [31]. A more detailed description of nanoparticle agglomeration processes can be found in [32]. To determine the chemical composition of the samples of obtained magnetite nanoparticles, elemental analysis was carried out using an energy-dispersive spectrometer. The energy-dispersive spectrum and the results of the study of the chemical composition are shown in Figure 3a. According to the results of the EDAX analysis, the mass fraction of iron (Fe) was 74.31% and the atomic fraction was 45.32%; the mass fraction of oxygen (O) was 25.69% and the atomic share was 54.68%. The X-ray pattern of magnetite nanoparticles, shown in Figure 3b, contains 9 diffraction peaks at the angles of 2θ = 18.5; 30.1; 35.5; 43.2; 53.6; 57.1; 62.7; 71.3, and 74.2 degrees, which correspond to the crystal planes of the magnetite phase

(111), (220), (311), (400), (422), (511), (440), (620), and (533), respectively [33]. According to the Scherrer equation, the average particle size, $t = \lambda/(\beta\cos\theta)$, can be estimated from the $CuK_\alpha(\lambda)$ X-ray wavelength, Bragg angle (θ), and the total peak width at half-height (β) in the radians. The size of synthesized magnetite particles, using the Scherrer equation, was 10.4 nm, which did not contradict the TEM image data.

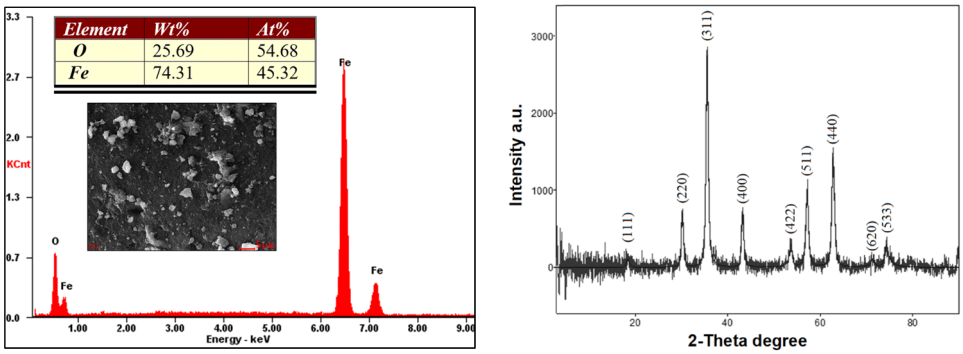

(**a**) (**b**)

Figure 3. (**a**) EDS spectrum and elemental composition, (**b**) X-ray diffraction pattern of magnetite nanoparticles.

The values of the magnetic moment of the obtained samples of magnetite nanoparticles were measured on a cryogenic magnetometer. The measurement results are shown in Figure 4. The studies performed showed that magnetite nanoparticles pass into the superparamagnetic state, as indicated by the absence of hysteresis in the field magnetization curve. The transition to the supermagnetic state is explained by the transition of magnetite nanoparticles to a single-domain state, and by the fact that uniform magnetization is achieved throughout the volume.

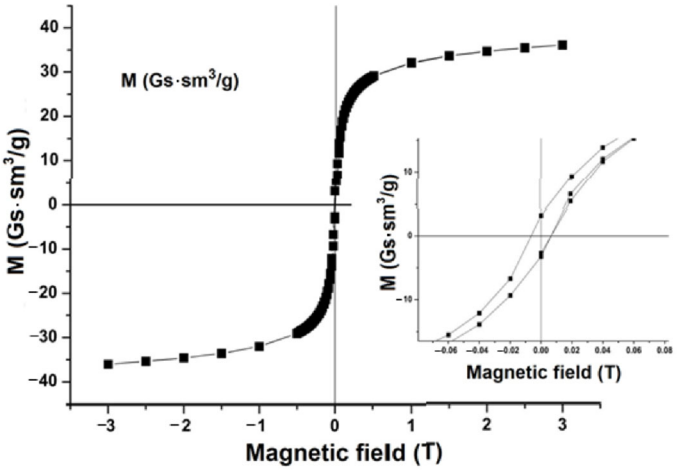

Figure 4. Magnetic hysteresis of magnetite nanoparticles at room temperature.

To investigate the structure and morphology, the obtained PAN/Fe_3O_4 fibers were examined using scanning electron microscopy and EDS analysis. For comparison, PAN fibers obtained at the same polymer concentrations and under the same conditions for the electrospinning process, but without magnetite, were also studied. Figure 5 shows the SEM image of the pure PAN fibers without magnetite, and Figure 6 shows PAN/Fe_3O_4 fibers.

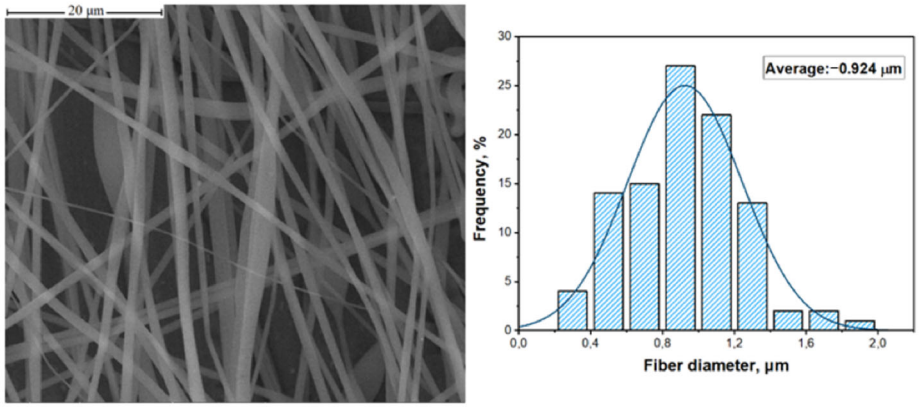

(**a**) (**b**)

Figure 5. (**a**) SEM image of pure PAN fibers; (**b**) distribution of PAN fibers according to diameter.

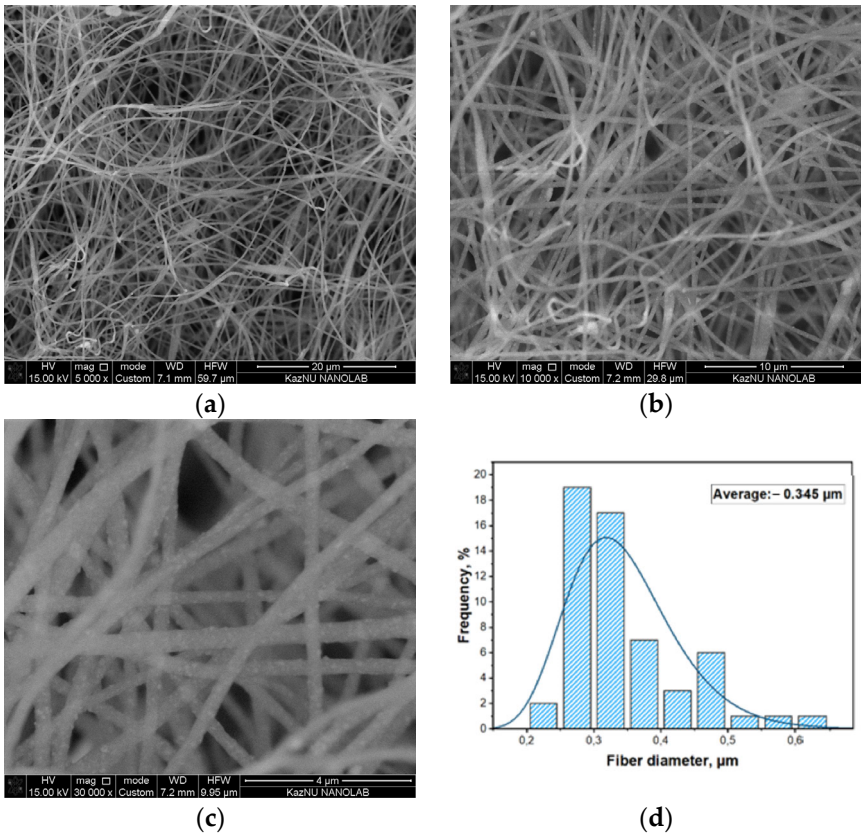

(**a**) (**b**)

(**c**) (**d**)

Figure 6. (**a**–**c**) SEM images of PAN/Fe_3O_4 fibers at various magnifications; (**d**) distribution of PAN/Fe_3O_4 fibers according to diameter.

PAN fibers synthesized without the addition of magnetite nanoparticles have a smooth surface without surface defects, open porosity, and clusters. The addition of magnetite to the solution resulted in a reduction in the diameter of the fibres formed as a result of electrospinning. In comparison for PAN fibres the diameter is 0.924 μm and for PAN/Fe_3O_4 fibres the diameter is 0.345 μm. A similar decrease in fiber diameter with the addition of magnetite was observed by the authors of [34], who obtained nanofibers based on polyvinyl alcohol and magnetite by electrospinning. Further, in [35], the authors investigated the inclusion of magnetite nanoparticles during the electrospinning of PAN fibers. The addition of 10, 25, and 40 wt. % of magnetite resulted in a decrease in diameter: 165, 139, and 74 nm, respectively. The authors explain this process through the effect of magnetite nanoparticles on the properties of the polymer

solution and the change in conductivity, viscosity, and surface tension. The authors in [34] experimentally found that increasing the magnetite content in the initial solution from 0.075 to 0.175 g led to a decrease in the fiber diameter from 186.5 to 131.4 nm and increases in saturation magnetization and residual magnetization. The obtained SEM images (see Figure 6) show a uniform distribution of magnetite nanoparticles over the entire fiber surface. Figure 7 shows the results of the elemental analysis of the composite fibers. High carbon content (65.95 wt. %) and a small amount of iron (9.33 wt. %) are observed, and nitrogen (17.49 wt. %) and oxygen (7.23 wt. %) are also present.

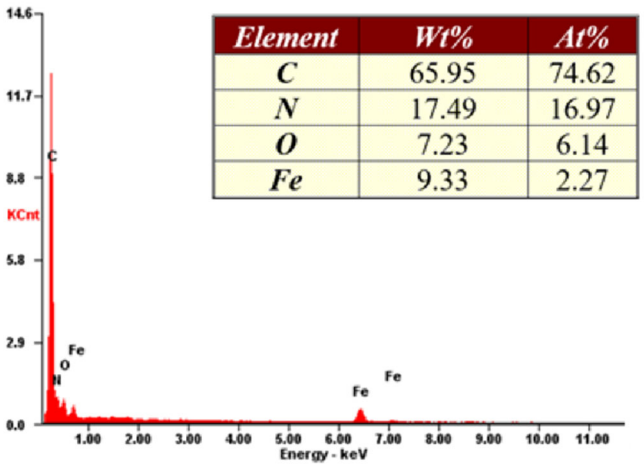

Element	Wt%	At%
C	65.95	74.62
N	17.49	16.97
O	7.23	6.14
Fe	9.33	2.27

Figure 7. EDS analysis of PAN/Fe_3O_4 fibers.

To detect a possible interaction between PAN polymer and magnetite nanoparticles during solution preparation and/or during the electrospinning of the fibers, PAN/Fe_3O_4-fibers were investigated using X-ray phase analysis.

According to the XRD results (Figure 8), it was found that the magnetite particles in the PAN-based fibers did not undergo any chemical transformation, retained their original chemical formula (Fe_3O_4) and crystal structure, and represented single-phase magnetite in the medium of the polymer matrix. It should be noted that there were peaks corresponding to the crystallites of silicon on the X-ray pattern since the sample was attached to a substrate of monocrystalline silicon during the analysis.

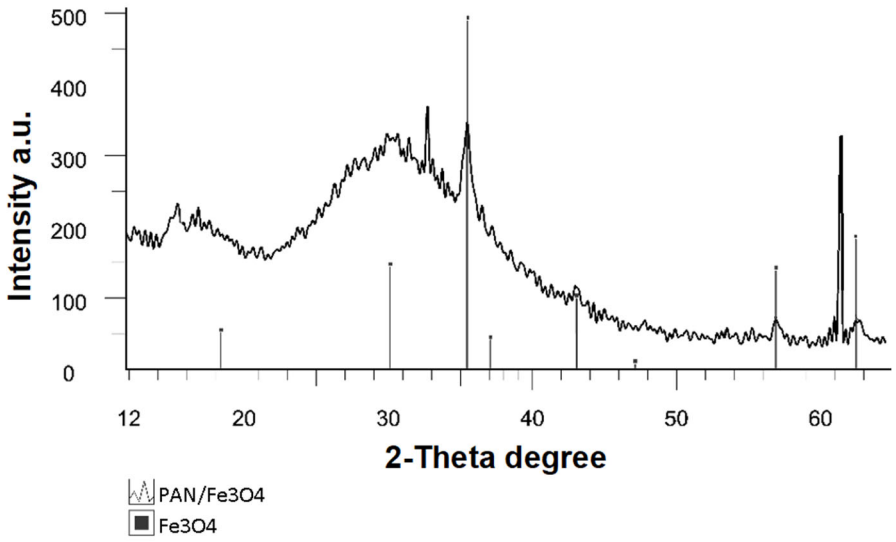

Figure 8. XRD patterns of PAN/Fe_3O_4 fibers.

Studies were performed on the synthesis of composite fibers from polyacrylonitrile with the addition of the magnetite nanoparticles obtained through chemical condensation. The method of electrospinning from the PAN solution in dimethylformamide with the addition of magnetite nanoparticles was applied to form the nanofibers. Depending on the field of practical application, composite fibers must have given characteristics of magnetite nanoparticle diameters and fibers, magnetite particle distribution on the surface and/or fiber structure, porosity, etc. The resulting fibers have the prospect of potential practical applications, such as for photovoltaics and photon sensing; the absorption of microwave and other radiation as a shield [36]; as a catalyst [37]; in wastewater treatment for heavy metal ions and organic pollutants; for drug delivery in biotechnology and biomedicine, in cell growth and tissue engineering; the creation of magnetic sensors [38,39]; as electrode material for lithium metal anodes [40], in medicine as a method of cancer treatment through magnetic hyperthermia [41], and as a biomedical adsorbent [42,43].

4. Conclusions

This study describes the results of experiments on the synthesis of magnetite nanoparticles through chemical condensation. Their average size was 10–12 nm, which was confirmed by the results of XRD, TEM, and SEM analyses. The magnetic properties of magnetite nanoparticles were studied. The studies performed showed that magnetite nanoparticles passed into the super-paramagnetic state, as indicated by the absence of hysteresis in the field magnetization curve. The transition to the supermagnetic state was explained by the transition of magnetite nanoparticles to a single-domain state, and by the fact that uniform magnetization was achieved throughout the volume. Magnetite nanoparticles were used to create composite PAN/Fe_3O_4 fibers by adding magnetite to the PAN solution to obtain a homogeneous suspension. Fibers were produced from a 7 wt. % PAN/Fe_3O_4 suspension in dimethylformamide through the electrospinning method. The SEM method showed that the magnetite nanoparticles were uniformly distributed throughout the fiber structure, with an average diameter of 0.345 μm. A comparison of PAN fibers without magnetite and PAN/Fe_3O_4 fibers showed that the addition of magnetite led to decreases in the diameters of the fibers at the same polymer concentrations and conditions of the electrospinning process. The resulting PAN/Fe_3O_4 composite fibres can be used in several practical applications, including sensors, magnetic materials, electronics, etc.

Author Contributions: Z.M., writing—reviewing and editing, G.S., data curation, writing—original draft preparation, B.K., visualization, investigation, A.I., conceptualization, methodology, software, A.L., writing—reviewing and editing. All authors have read and agreed to the published version of the manuscript.

Funding: This research was funded by the Committee of Science of the Ministry of Education and Science of the Republic of Kazakhstan, grant number and title: "OR11465430 Development of new composite and structural materials for the development of the innovative industry of the Republic of Kazakhstan" under the subprogram "Development of technology for obtaining carbon fibers and their application as sensors and carbon composite material".

Institutional Review Board Statement: Not applicable.

Informed Consent Statement: Not applicable.

Data Availability Statement: The data presented in this study are available upon request from the corresponding author.

Conflicts of Interest: The authors declare no conflict of interest.

References

1. Gloag, L.; Mehdipour, M.; Chen, D.; Tilley, R.D.; Gooding, J.J. Advances in the Application of Magnetic Nanoparticles for Sensing. *Adv. Mater.* **2019**, *31*, e1904385. [CrossRef] [PubMed]
2. Subramanian, A.S.; Meenalochini, P.; Sathiya, S.S.B.; Prakash, G.R. A review on selection of soft magnetic materials for industrial drives. *Mater. Today Proc.* **2021**, *45*, 1591–1596. [CrossRef]

3. Wang, B.; Liu, Q.; Fan, Z. A mini review: Application progress of magnetic graphene three-dimensional materials for water purification. *Front. Chem.* **2020**, *8*, 595643. [CrossRef] [PubMed]
4. Hossain, M.; Qin, B.; Li, B.; Duan, X. Synthesis, characterization, properties and applications of two-dimensional magnetic materials. *Nano Today* **2022**, *42*, 101338. [CrossRef]
5. Kaur, B.; Kaushal, G.; Rana, S.; Kumar, P.; Khanra, P.; Dhiman, M. Magnetic Ferrites: A Brief Review About Substation on Electric and Magnetic Properties. *ECS Trans.* **2022**, *107*, 9093. [CrossRef]
6. Zhou, K.; Zhou, X.; Liu, J.; Huang, Z. Application of magnetic nanoparticles in petroleum industry: A review. *J. Pet. Sci. Eng.* **2020**, *188*, 106943. [CrossRef]
7. Zhou, Y.; Yu, W.; Khan, A.; Chong, X.; Feng, J. The investigation on structural, electronic, elastic, adsorptive, catalytic and magnetic properties of precious metal materials via first-principles calculations based on density functional theory—A review. *J. Micromechanics Mol. Phys.* **2020**, *5*, 2030001. [CrossRef]
8. Wu, K.; Su, D.; Liu, J.; Saha, R.; Wang, J.-P. Magnetic Nanoparticles in Nanomedicine: A Review of Recent Advances. *Nanotechnology* **2019**, *30*, 502003. [CrossRef]
9. Mylkie, K.; Nowak, P.; Rybczynski, P.; Ziegler-Borowska, M. Polymer-Coated Magnetite Nanoparticles for Protein Immobilization. *Materials* **2021**, *14*, 248. [CrossRef]
10. Mikhailov, Y.M.; Aleshin, V.V.; Zhemchugova, L.V.; Kovalev, D.Y. Transformations of Iron (III) Precursors in a Wave of Flameless RDX Combustion. *Int. J. Self-Propagating High-Temp. Synth.* **2018**, *27*, 162–166. [CrossRef]
11. Arévalo-Cid, P.; Isasi, J.; Martín-Hernández, F. Comparative Study of Core-Shell Nanostructures Based on Amino-Functionalized Fe_3O_4@SiO_2 and $CoFe_2O_4$@SiO_2 Nanocomposites. *J. Alloys Compd.* **2018**, *766*, 609–618. [CrossRef]
12. Katz, E. Synthesis, Properties and Applications of Magnetic Nanoparticles and Nanowires—A Brief Introduction. *Magnetochemistry* **2019**, *5*, 61. [CrossRef]
13. Evdokimov, S.I.; Pan'shin, A.M.; Kanashvili, M.Z. Magnetic Fluid: New Technology. *Russ. J. Non-Ferr. Met.* **2008**, *49*, 78–81. [CrossRef]
14. Han, C.; Cai, W.; Tang, W.; Wang, G.; Liang, C. Protein Assisted Hydrothermal Synthesis of Ultrafine Magnetite Nanoparticle Built-Porous Oriented Fibers and Their Structurally Enhanced Adsorption to Toxic Chemicals in Solution. *J. Mater. Chem.* **2011**, *21*, 11188. [CrossRef]
15. Mamun, A.; Sabantina, L.; Klöcker, M.; Heide, A.; Blachowicz, T.; Ehrmann, A. Electrospinning Nanofiber Mats with Magnetite Nanoparticles Using Various Needle-Based Techniques. *Polymers* **2022**, *14*, 533. [CrossRef]
16. Darwish, M.S.A.; Bakry, A.; Kolek, O.; Martinová, L.; Stibor, I. Electrospun functionalized magnetic polyamide 6 composite nanofiber: Fabrication and stabilization. *Polym. Compos.* **2019**, *40*, 296–303. [CrossRef]
17. Wang, B.; Sun, Y.; Wang, H. Preparation and Properties of Electrospun PAN/Fe_3O_4 Magnetic Nanofibers. *J. Appl. Polym. Sci.* **2010**, *115*, 1781–1786. [CrossRef]
18. Fokin, N.; Grothe, T.; Mamun, A.; Trabelsi, M.; Klöcker, M.; Sabantina, L.; Döpke, C.; Blachowicz, T.; Hütten, A.; Ehrmann, A. Magnetic Properties of Electrospun Magnetic Nanofiber Mats after Stabilization and Carbonization. *Materials* **2020**, *13*, 1552. [CrossRef]
19. Zhu, J.; Wei, S.; Rutman, D.; Haldolaarachchige, N.; Young, D.P.; Guo, Z. Magnetic Polyacrylonitrile-Fe@FeO Nanocomposite Fibers—Electrospinning, Stabilization and Carbonization. *Polymer* **2011**, *52*, 2947–2955. [CrossRef]
20. Storck, J.L.; Grothe, T.; Mamun, A.; Sabantina, L.; Klöcker, M.; Blachowicz, T.; Ehrmann, A. Orientation of Electrospun Magnetic Nanofibers Near Conductive Areas. *Materials* **2019**, *13*, 47. [CrossRef]
21. Liu, G.-L.; Zhang, Y.-M.; Tian, D.; Zhou, B.-Z.; Lu, Z.-Q.; Wang, C.-X. Last Patents on Bubble Electrospinning. *Recent Pat. Nanotechnol.* **2020**, *14*, 5–9. [CrossRef] [PubMed]
22. Shakil, U.A.; Bin Abu Hassan, S.; Yahya, M.Y.; Rejab, M.R.M. A focused review of short electrospun nanofiber preparation techniques for composite reinforcement. *Nanotechnol. Rev.* **2022**, *11*, 1991–2014. [CrossRef]
23. Furlan, D.M.; Morgado, D.L.; de Oliveira, A.J.A.; Faceto, Â.D.; de Moraes, D.A.; Varanda, L.C.; Frollini, E. Sisal Cellulose and Magnetite Nanoparticles: Formation and Properties of Magnetic Hybrid Films. *J. Mater. Res. Technol.* **2019**, *8*, 2170–2179. [CrossRef]
24. Xia, S.; Song, L.; Hohn, N.; Wang, K.; Grott, S.; Opel, M.; Schwartzkopf, M.; Roth, S.V.; Müller-Buschbaum, P. Spray-Coating Magnetic Thin Hybrid Films of PS-*b*-PNIPAM and Magnetite Nanoparticles. *Adv. Funct. Mater.* **2019**, *29*, 1808427. [CrossRef]
25. Ganonyan, N.; He, J.; Temkin, A.; Felner, I.; Gvishi, R.; Avnir, D. Ultralight Monolithic Magnetite Aerogel. *Appl. Mater. Today* **2021**, *22*, 100955. [CrossRef]
26. Raju, R.R.; Liebig, F.; Klemke, B.; Koetz, J. Ultralight Magnetic Aerogels from Janus Emulsions. *RSC Adv.* **2020**, *10*, 7492–7499. [CrossRef]
27. Kostishyn, V.G.; Ostafiychuk, B.K.; Moklyak, V.V.; Nuriev, A.V. Mossbauer Investigation of Magnetic Polymer Nanocomposites Based on Magnetite And Polyvinyl Alcohol. *Izv. Vyss. Uchebnykh Zaved. Mater. Elektron. Tekhniki Mater. Electron. Eng.* **2015**, *4*, 22. [CrossRef]
28. Lesbayev, A.; Elouadi, B.; Borbotko, T.; Manakov, S.; Smagulova, G.; Boiprav, O.; Prikhodko, N. Influence of Magnetite Nanoparticles on Mechanical and Shielding Properties of Concrete. *Eurasian Chem.-Technol. J.* **2017**, *19*, 223–229. [CrossRef]
29. Lesbayev, A.B.; Elouadi, B.; Lesbayev, B.T.; Manakov, S.M.; Smagulova, G.T.; Prikhodko, N.G. Obtaining of Magnetic Polymeric Fibers with Additives of Magnetite Nanoparticle. *Procedia Manuf.* **2017**, *12*, 28–32. [CrossRef]

30. Mansurov, Z.A. Recent Achievements and Future Challenges in Nanoscience and Nanotechnology. *Eurasian Chem.-Technol. J.* **2020**, *22*, 241. [CrossRef]
31. Darwish, M.S.A.; Bakry, A.; Al-Harbi, L.M.; Khowdiary, M.M.; El-Henawy, A.A.; Yoon, J. Core/shell PA6@ Fe3O4 nanofibers: Magnetic and shielding behavior. *J. Dispers. Sci. Technol.* **2020**, *11*, 1711–1719. [CrossRef]
32. Yeap, S.P.; Lim, J.; Ooi, B.S.; Ahmad, A.L. Agglomeration, colloidal stability, and magnetic separation of magnetic nanoparticles: Collective influences on environmental engineering applications. *J. Nanoparticle Res.* **2017**, *19*, 368. [CrossRef]
33. International Centre for Diffraction Data. JCPDS Card 03–065–3107. International Centre for Diffraction Data: Newtown Square, PA, USA. Available online: https://www.icdd.com/ (accessed on 5 October 2022).
34. Taufiq, A.; Ainun Jannah, M.; Hidayat, A.; Hidayat, N.; Mufti, N.; Munasir; Susanto, H. Structural and Magnetic Behaviours of Magnetite/Polyvinyl Alcohol Composite Nanofibers. *IOP Conf. Ser. Mater. Sci. Eng.* **2019**, *515*, 012081. [CrossRef]
35. Sabzroo, N.; Rohani Bastami, T.; Karimi, M.; Heidari, T. Optimization of electrospinning conditions for magnetic poly (acrylonitrile-co-acrylic acid) nanofibers. *J. Nanostructures* **2019**, *9*, 301–315. [CrossRef]
36. Zhan, Y.; Long, Z.; Wan, X.; Zhang, J.; He, S.; He, Y. 3D carbon fiber mats/nano-Fe_3O_4 hybrid material with high electromagnetic shielding performance. *Appl. Surf. Sci.* **2018**, *444*, 710–720. [CrossRef]
37. Apler, A.; Snowball, I.; Frogner-Kockum, P.; Josefsson, S. Distribution and dispersal of metals in contaminated fibrous sediments of industrial origin. *Chemosphere* **2019**, *215*, 470–481. [CrossRef]
38. Gan, Y.; Yu, C.; Panahi, N.; Gan, J.; Cheng, W. Processing Iron Oxide Nanoparticle-Loaded Composite Carbon Fiber and the Photosensitivity Characterization. *Fibers* **2019**, *7*, 25. [CrossRef]
39. Blachowicz, T.; Ehrmann, A. Most Recent Developments in Electrospun Magnetic Nanofibers: A Review. *J. Eng. Fibers Fabr.* **2020**, *15*, 155892501990084. [CrossRef]
40. Chen, H.; Li, M.; Li, C.; Li, X.; Wu, Y.; Chen, X.; Wu, J.; Li, X.; Chen, Y. Electrospun carbon nanofibers for lithium metal anodes: Progress and perspectives. *Chin. Chem. Lett.* **2021**, *33*, 141–152. [CrossRef]
41. Matos, R.J.R.; Chaparro, C.I.P.; Silva, J.C.; Valente, M.A.; Borges, J.P.; Soares, P.I.P. Electrospun composite cellulose acetate/iron oxide nanoparticles non-woven membranes for magnetic hyperthermia applications. *Carbohydr. Polym.* **2018**, *198*, 9–16. [CrossRef]
42. Hu, Q.-L.; Wang, L.-S.; Yu, N.-N.; Zhang, Z.-F.; Zheng, X.; Hu, X.-M. Preparation of Fe_3O_4@C@TiO_2 and its application for oxytetracycline hydrochloride adsorption. *Rare Met.* **2020**, *39*, 1333–1340. [CrossRef]
43. Song, J.; Guan, R.; Xie, M.; Dong, P.; Yang, X.; Zhang, J. Advances in electrospun TiO_2 nanofibers: Design, construction, and applications. *Chem. Eng. J.* **2021**, *431*, 134343. [CrossRef]